IIETA International Information and Engineering Technology Association
Advancing the World of Information and Engineering

Journal Européen des Systèmes Automatisés
Vol. 55, No. 5, October, 2022, pp. 623-631
Journal homepage: http://iieta.org/journals/jesa

Energy Management of a Hybrid Generation System Based on Wind Turbine Coupled with a Battery/Supercapacitor

Yazid Sadok Bouziane[1], Noureddine Henini[2*], Abdelhalim Tlemçani[1]

[1] Electrotechnics and Automation Research Laboratory, University of Medea, Medea 26000, Algeria
[2] Renewable Energy and Materials Laboratory, University of Medea, Medea 26000, Algeria

Corresponding Author Email: n.d.henini@gmail.com

https://doi.org/10.18280/jesa.550507

Received: 18 August 2022
Accepted: 16 October 2022

Keywords:
hybrid generation system, wind turbine, permanent magnet synchronous generator, battery, supercapacitor, energy management

ABSTRACT

In this paper, an energy management method for a stand-alone hybrid generation system based on a wind turbine and hybrid energy storage system (battery/supercapacitor). The supercapacitor is included to reduce the transient peak energy caused by sudden load or wind speed variations and reduce battery charging stress. Consequently, it extends battery life and reduces replacement costs. The power management method is introduced to maintain the necessary energy balance between the sides of generation and load. Additionally, a wind boost converter is present to harness the most wind energy possible while meeting load requirements and preserving a constant DC-bus voltage. The simulation results demonstrate how quickly the suggested technique can adapt to wind speed and load power changes.

1. INTRODUCTION

In the recent years, renewable energy systems, such as wind turbines, biofuels, and photovoltaics, have been widely used to raise electricity demand and reducing environmental deterioration [1]. Globally, the production of renewable energy climbed by 7% in 2018 [2] and is projected to account for 63% of global energy demand by 2050 [3]. In particular, wind energy supplied 7% of the world's energy needs in 2018 [2] and will account for 24% by 2050 [3]. However, the usage of renewable energy is constrained by intermittent and unpredictable uncertainty in these sources. Hybrid systems are used to increase the utilization of renewable energy as well as to combine the advantages of the different types of multi-energy storage systems (ESS).

For example, a significant number of academic studies that have lately been implemented, or proposed, show the growing interest in linked renewable energy and energy storage technologies [4, 5]. Hybrid compressed air energy storage, wind and geothermal energy systems are studied by Rahmanifard and Plaksina [6]. Another case studied the operation of a photovoltaic-wind plant with hydro-pumping storage for electricity peak shaving [7]. An energy management study deals with the modelling and control of a hybrid power system containing a fuel cell and a wind turbine (WT) system based on a Doubly Fed Induction Generator (DFIG) with a Super Capacitor Storage System [8]. Another type of energy storage based on flywheels is dedicated to improving the quality of energy with advanced control for wind energy conversion systems is studied by Hamzaoui et al. [9].

Wind energy is treated as the fastest growing and most promising renewable energy resource around the world. However, the variable nature of wind and unsteady load profiles create the operation of wind-based power systems difficult, significantly once they operate in standalone mode [10]. Fluctuation in the output power of a wind turbine as a result of the variable nature of wind speed, tower shadow, and wind shear can cause voltage flicker [11], which in turn can affect the frequency response of the system [12].

Since the main problem with wind generators is the high coupling between the generated power and the actual wind speed, one interesting solution is the use of a hybrid energy storage system (ESS) that controls the power flow between the generator and the consumption side [13]. In addition, the ESS can be controlled to provide power regulation and load voltage control [14].

A stand-alone wind-based power system with a hybrid energy storage system based on batteries and supercapacitors is proposed in this paper. The wind turbine is based on a permanent magnet synchronous generator (PMSG) [15]. The benefits of PMSG include higher efficiency, gear-free transmission, high reliability, effective control, Maximum Power Point Tracking (MPPT) capability, and reduced noise emissions, among others [16]. The energy flow control strategy established uses the maximum power point tracking (MPPT) control algorithm to maximize the wind-captured energy, maintain system stability, and remove the impact of power transients on the battery's life [17].

The principal idea in the energy management strategy is that the batteries are used to provide a consistent energy supply, and the SCs, due to their high-power density and quick response, provide the instantaneous peak power during transients. This strategy can reduce the battery's capacity, extend its lifespan, lower the replacement cost, and improve system reliability [18]. This research examines the performance of a hybrid system's parts under varying wind and load circumstances. The energy management strategy should be in place to coordinate power sharing between the battery and the SC and maintain power balance between the sides of generation and consumption [19].

2. PROPOSED SYSTEM MODELLING

Figure 1 depicts the proposed wind power system coupled with the hybrid ESS (battery/supercapacitor). To supply a variable AC load, the system components are connected to a common 350V DC-bus through DC/DC and AC/DC converters.

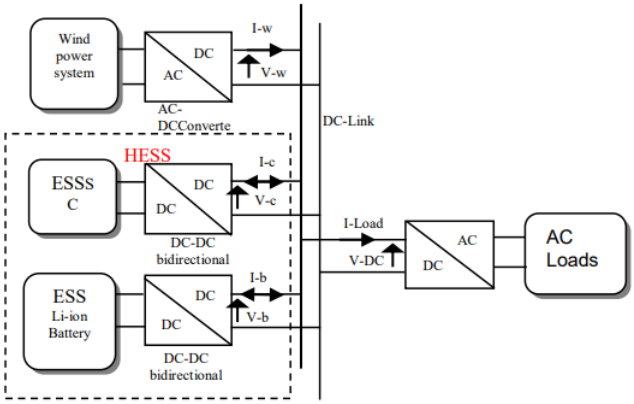

Figure 1. Hybrid generation system proposed

2.1 Wind energy conversion system

Figure 2 depicts the proposed wind power system's schematic.

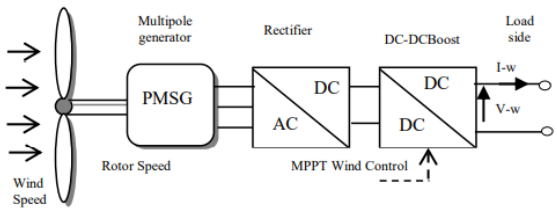

Figure 2. Wind turbine scheme

The wind turbine's output can be expressed mathematically as [20]:

$$P_w = \frac{1}{2}\rho\pi R^2 V_w^3 C_p(\lambda,\beta) \tag{1}$$

where, ρ is the air density, R the turbine's radius,V_w the wind speed expressed in meters per second, and C_p the power coefficient, which is influenced by the pitch angle and tip speed ratio [21, 22].

The tip speed ratio is given by:

$$\lambda = \frac{W_r . R}{V_w} \tag{2}$$

where, W_r is the turbine angular speed.

The power coefficient C_p is defined by [16]:

$$C_p(\lambda,\beta) = C_1\left(\frac{C_2}{\lambda_i} - C_3\beta - C_4\right)e^{-\left(\frac{C_5}{\lambda_i}\right)} + C_6\lambda \tag{3}$$

$$\frac{1}{\lambda_i} = \frac{1}{\lambda + 0.08\beta} - \frac{0.035}{1+\beta^3} \tag{4}$$

The constants C_1 to C_6 are obtained through experimental tests [21].

A permanent magnet synchronous generator (PMSG) is a variable speed wind energy conversion system. It is employed in the process of converting mechanical energy into electrical energy.

The equations below use Park transformation to model the PMSG [23].

$$V_{sd} = R_s i_d + \frac{d\lambda_d}{dt} - w_e\lambda_q \tag{5}$$

$$V_{sd} = R_s i_q + \frac{d\lambda_q}{dt} - w_e\lambda_d \tag{6}$$

where, R_s is the resistance of the stator winding, V_{sd} and V_{sq} are the stator voltages, and i_d and i_q are the stator currents in the d-q reference frame.

The components of stator flux are given by:

$$\lambda_d = L_{sd} i_d + \lambda_m, \qquad \lambda_q = L_{sq} i_q \tag{7}$$

where, L_{sd}, L_{sq} are the d-q inductances of the stator winding and λ_m is the core magnetic flux.

The following equation can be used to calculate the PMSG electrical torque:

$$T_e = \frac{3}{2}p\left[\lambda_m i_q - (L_{sq} - L_{sd}) i_q i_d\right] \tag{8}$$

where, p is a pair of PMSG poles.

L_{sd} and L_{sq} are equal for the surface-mounted magnet machine type.

The electrical torque is [24]:

$$T_e = \frac{3}{2}p(\lambda_m i_q) \tag{9}$$

2.2 Energy storage system ESS

The hybrid ESS components used are: A 240V, 75Ah lithium-ion battery, A 350V, 30F supercapacitor.

The battery types are preferred over others because of their excellent resistance to climatic fluctuations and lengthy anticipated lifetime [25].

A bidirectional converter connects each hybrid ESS element to the 350V DC-bus. The bidirectional converter functions as a buck converter in charging mode to transfer energy from the higher voltage side (DC-bus) to the lower voltage side (ESS device). In discharging mode, it functions as a boost converter.

$$\text{Buck mode: } V_0 = \alpha V_i \tag{10}$$

$$\text{Boost mode: } V_0 = V_i/(1-\alpha) \tag{11}$$

where, V_0, V_i, and α, respectively, are the output voltage, input voltage, and duty cycle of the DC/DC converter.

2.3 Sizing of battery and supercapacitor

The supercapacitor is intended to function as a component of the ESS, but its primary function is to mitigate huge power variations that a battery is ill-equipped to handle during charge/discharge. The supercapacitor must be able to handle the peak current that travels between the ESS and DC-link in order to do this. To select the proper supercapacitor size in respect of power (the peak current is important), we have to consider the following [26]:

$$i(t) = C_{SC}\frac{dV(t)}{\mathrm{dt}} \tag{12}$$

$$P(t) = V(t).i(t) \tag{13}$$

The following (14) and (15) are required in order to choose the best supercapacitor size in terms of energy.

The stored energy in the supercapacitor can be calculated as follows:

$$\mathrm{E_{ex}} = \int_0^{\tau} P(t).dt \tag{14}$$

$$E = 0.5\ C_{SC}\mathrm{V}^2 \tag{15}$$

The supercapacitor's highest voltage drop may reach 80% of its maximum voltage.

The supercapacitor's maximum exchanged energy is determined as indicated in (16):

$$\mathrm{E_{max-ex}} = 0.5\ C_{SC}{V_{max}}^2 - 0.5\ C_{SC}{V_{min}}^2 \tag{16}$$

where, $\mathrm{V_{max}}$ and $\mathrm{V_{min}}$ are maximum and minimum allowable voltage of supercapacitor, respectively. The supercapacitor's maximum permissible exchanged energy, $\mathrm{E_{max-ex}}$, impacts its state of charge (SOC), and as it rises, a battery's operational time reduces. Smaller batteries are designed as a result of the supercapacitor's larger permitted energy exchange. The right battery size relates to the rated power of the turbine. DC-link's voltage and the ratio of low wind speed time duration with respect to the total time duration (LWD) as shown in (17).

$$C_{batt} \infty \frac{P_{wt}\ .\ LWD\ .V_{dc-link}}{C_{SC}} \tag{17}$$

The rated power of the turbine, the voltage of the DC-link, and the wind speed profile (Wind speed is unpredictable, but we can determine the range of wind speed fluctuation based on historical data) affect ESS capacity.

The following factors must be taken into account when determining the size of a supercapacitor: variations in wind speed and power generated by the wind, battery power density, and DC-link voltage.

We require a greater supercapacitor capacity if the percentage of high magnitude variations in the generated power is high.

The final capacity of the supercapacitor is obtained by multiplying the calculated capacity by a safety factor (for instance, 10% of the total capacity).

The energy that can be stored in the HESS is calculated, as shown in (18).

$$\mathrm{E_{HESS}} = P_{rated,\ turb} * t * 10\% \tag{18}$$

"t" is a time duration and "A" percent of $\mathrm{E_{HESS}}$ is related to the supercapacitor's capacity, as shown in (19).

$$\mathrm{E_{CS}} = \mathrm{E_{HESS}} * \mathrm{A}\% \tag{19}$$

As shown in (20), the size of the supercapacitor can be estimated (Supercapacitor is connected to DC-link in parallel, so that they have the same voltage) [26].

$$C = \frac{2\mathrm{E_{CS}}}{\mathrm{V}^2} \tag{20}$$

The size of the supercapacitor must be big enough to handle the high fluctuations in generated wind power.

3. CONTROL STRATEGIES

The following energy management solutions are suggested to accomplish the system's energy balance and maximize the efficiency of wind energy.

3.1 Wind energy system control

An MPPT controller is used to regulate the wind boost converter to accurately extract the maximum wind power under diverse wind speed scenarios. A Perturb and Observe MPPT algorithm is used in this paper. This method calculates the duty cycle of a DC-DC converter in the function of the output power [21]. The P&O algorithm's flowchart is depicted in Figure 3.

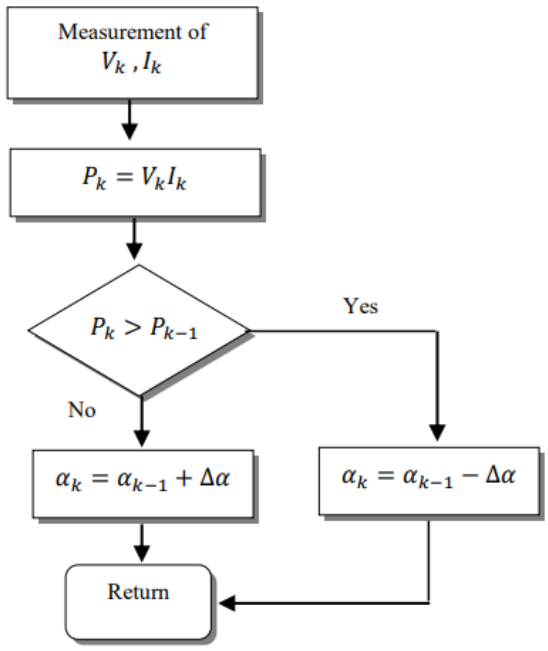

Figure 3. P&O flowchart

However, when the wind system power ($\mathrm{P_{wind}}$) > ($\mathrm{P_{Load}}$), even if the battery is fully charged, the extra power will be sent to it. The battery would deteriorate as a result. So, as depicted in Figure 4, an improvement is suggested to address this issue. The MPPT is disengaged, and the DC-bus voltage ($\mathrm{V_{DC}}$) regulation loop is turned on when a battery is fully charged (state of charge SOC reaches the maximum level).

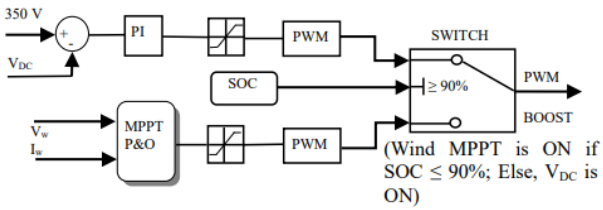

Figure 4. Wind DC/DC control scheme

3.2 Hybrid ESS control

In a stand-alone wind system, the hybrid ESS (battery/supercapacitor) is used to preserve the reliability of the power supply. Supercapacitors (SC), which have quick charge/discharge rates, can retain transient energy peaks, which reduces the capacity needed for batteries, lengthens their lifespan, and lowers the cost of replacement [27]. To do this, the power flow between the wind power generating and consumption sides will be separated into two components: the low-frequency component (LFC) and the transient high-frequency component (THFC). The SC will handle the latter while the battery is in charge of the LFC [28].

As depicted in Figure 5, the control method proposed has three control loops. First is the DC-link voltage control loop to keep the DC-bus voltage at 350V. This loop's output, the total reference current (I_{ref}), should be adjusted to account for any voltage drift. I_{ref} divides into two parts simultaneously, LFC and HFC. To extract its LFC which will serve as the reference to the second loop, the battery loop, it will first pass through a low pass filter. With the latter, the battery can account for LF's average degree of power drift. The third loop, or supercapacitor control loop, on the other hand, compensates the HFC of current.

Every loop covered in this paper runs into a PI controller. Moreover, Pulse width modulation (PWM) gated pulse for power electronics converters, technique is applied to the battery loop output to create the switch gating signals for the battery bidirectional converter. While $S_{(B-2)}$ is enabled for discharging, $S_{(B-1)}$ is activated for charging. Similar to this, gating signals for SC bidirectional converter switches ($S_{(SC-1)}$ for charging and $S_{(SC-2)}$ for discharging) are generated after PWMof the SC loop output.

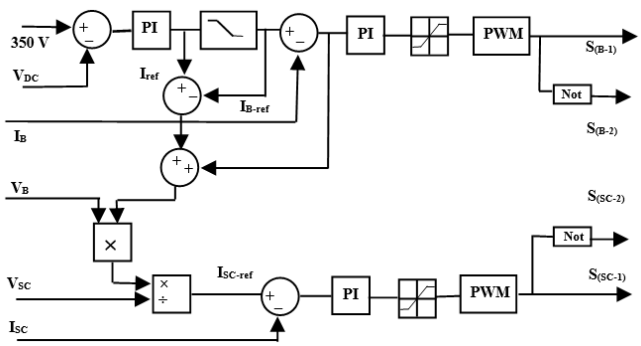

Figure 5. Hybrid ESS control scheme

4. SIMULATION RESULTS AND DISCUSSION

An 8.5 KW wind turbine power generator is used for simulation. Turbine output power curves for different wind speed conditions are shown in Figure 6.

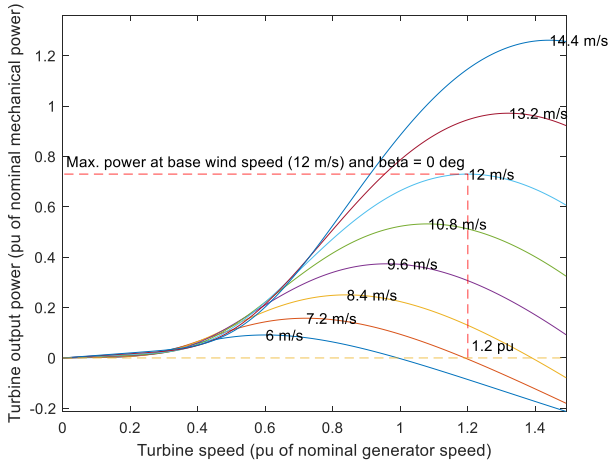

Figure 6. Wind turbine power characteristics

The proposed wind energy system combined with a battery/supercapacitor ESS effectiveness is verified using MATLAB/Simulink platform under different scenarios of load and wind speed variations.

4.1 Case 1: Variable wind speed and constant load power

In this case, the wind speed varies from $5m/s$ (at t=0.5s) to $12m/s$ (at $t \approx 1s$), and then from $12m/s$(at t=3s) to $9m/s$ (at $t \approx 3.5s$). The load power is 4000W, the wind velocity, the power from the wind system (P-wind), the load power (P-Load), the battery/SC charging-discharging power, SOC and the DC bus voltage are shown in Figures 7, 8, 9, 10, 11, 12, respectively.

4.2 Case 2: Variable load power and constant wind speed

The load power varies from 5000 to 1500W at t=1.75s, and then backwards from 1500W to 5000W at t=3.5s.

The wind speed is $12\ m/s$. Waveforms of the power from the wind turbine (P-wind), the load power demand (P-load), the battery and the supercapacitor (P-Bat/P-SC), the battery SOC the DC bus voltage is shown in Figures 13, 14, 15, 16, 17, respectively.

The primary goal is to keep the DC-link voltage at 350V and meet the load requirement regardless of changes in the load or wind speed. The battery should not be harmed by transients or overcharging for this to happen.

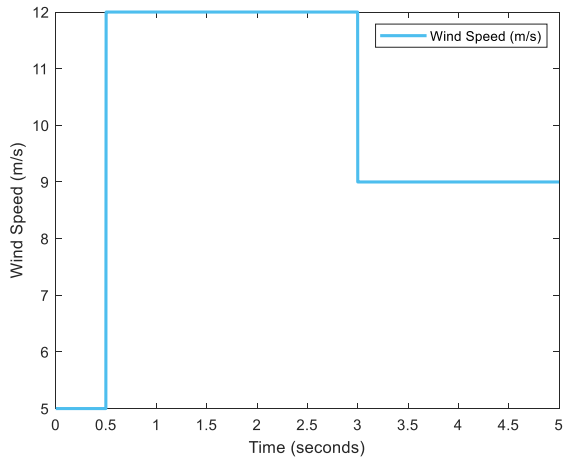

Figure 7. Wind speed variation

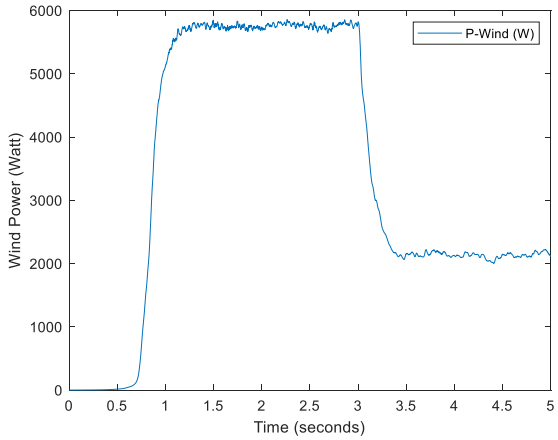

Figure 8. Wind system power

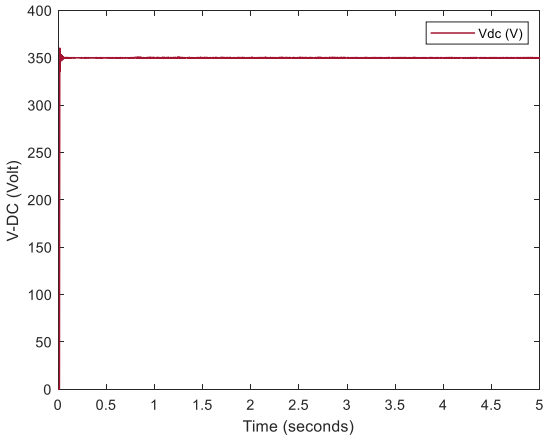

Figure 12. DC-Bus voltage

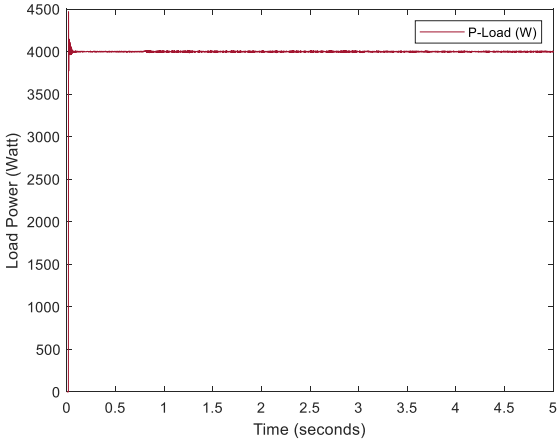

Figure 9. Load power

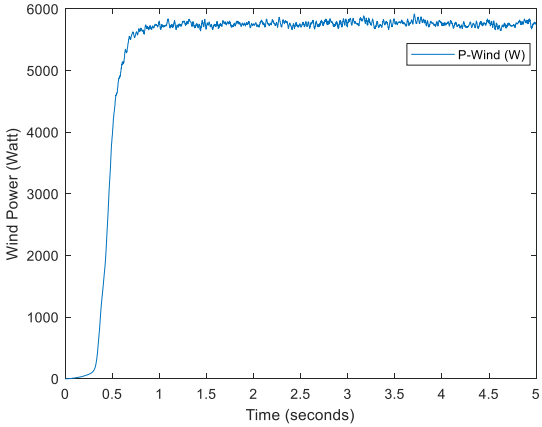

Figure 13. Wind power

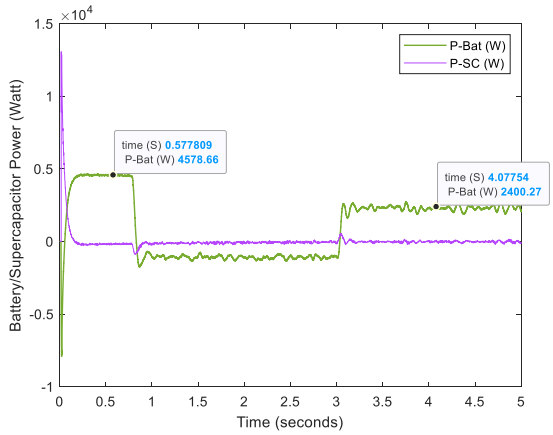

Figure 10. Hybrid ESS power

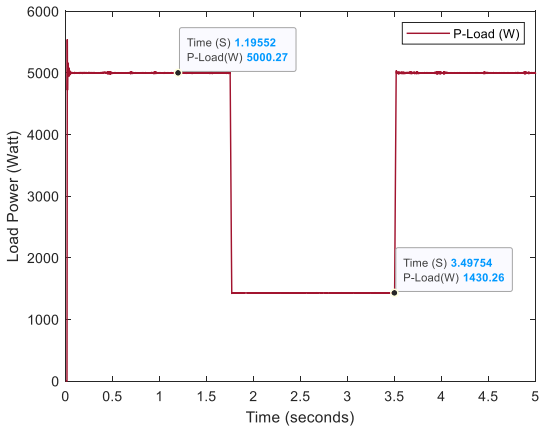

Figure 14. Load power

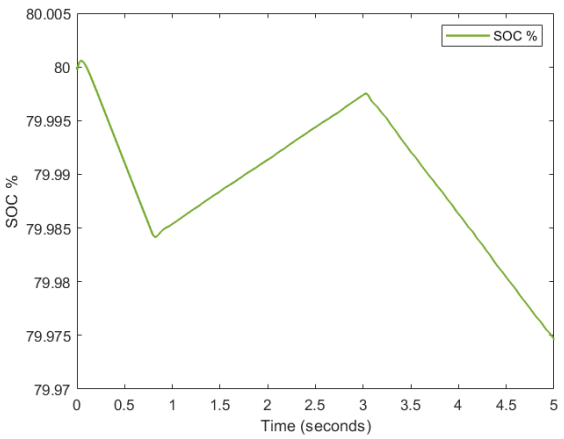

Figure 11. Battery SOC

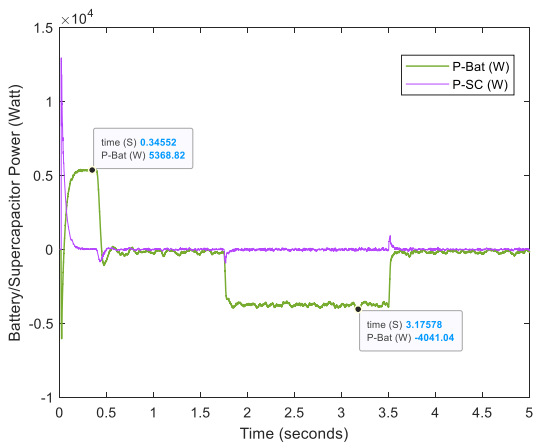

Figure 15. Hybrid ESS power

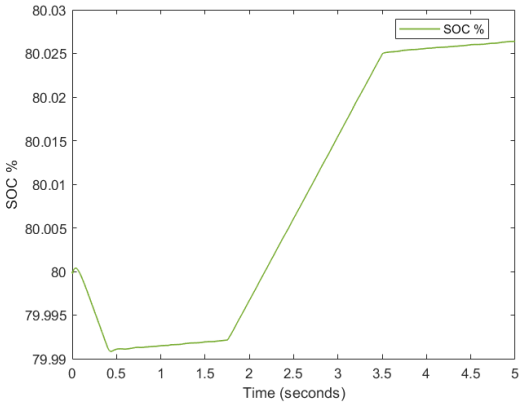

Figure 16. Battery SOC

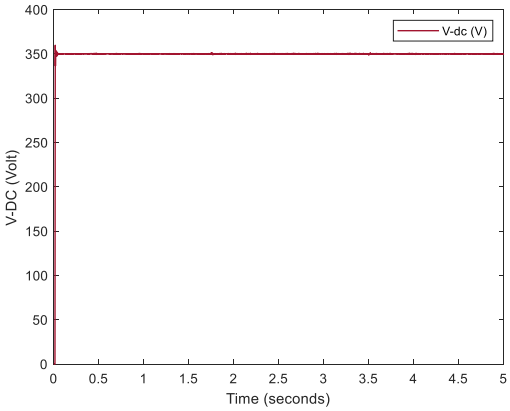

Figure 17. DC-Bus voltage

The DC connection voltage is successfully regulated at 350V, as shown in Figures 12 through 17. The maximum wind power was precisely tracked based on wind velocity, as seen in Figures 8 and 13.

Figure 9 and Figure 14 depicts the load demand and how it abruptly decreased from 5000 W to 1500 W in the second scenario (case 2) at $t = 1.75$s before returning to 5000 W at $t = 3.5$s, P-Load is constant in the first scenario (case 1) at 4000 W.

Figure 10 and Figure 15 demonstrate the supercapacitor's quick response in compensating transient peak powers during load or wind velocity variations, reducing battery charging stresses, and extending the battery's lifespan to take the lead in making up for any constant drift between generator and load powers.

The battery's state of charge (SOC) percentage is depicted in Figure 11 and Figure 16, and it changes based on the amount of wind energy and the load demand. The analysis of simulation results of wind power generation system and battery (case 1, 2), are presented in Table 1.

It can be seen from an analysis of the wind, load, and battery power data that the required energy balance is always maintained, and the load is always satisfied.

4.3 Case 3: Wind power system and Battery ESS

In this case, we use only the battery as an energy storage system instead of the Battery/SCs ESS.

The wind speed varies as in case 1, we suppose the load power constant at 4000 Watt.

Table 1. The results analysis description (case 1, 2)

Duration	Parameters	Results
Case 1 (From t=0 to t=0.5 sec)	Wind velocity:5m/s $P_{Load} = 4000$ W $P_{Wind} < P_{Load}$ Battery in discharging mode	Wind power is too low $P_{Battery} = 4518$ W load power is 4000 W (Surplus power 518 W)
Case 1 (From t=1 to t=3sec)	Wind velocity:12m/s $P_{Load} = 4000$ W $P_{Wind} > P_{Load}$ Battery in charging mode	Wind power is 5915 W $P_{Battery} = 1418$ W load power is 4000 W (Surplus power 497 W)
Case 1 (From t=3.5 to t=5 sec)	Wind velocity: 9m/s $P_{Load} = 4000$ W $P_{Wind} < P_{Load}$ Battery in discharging mode	Wind power is 2100 W $P_{Battery} = 2400$W load power is 4000W (Surplus power 500W)
Case 2 (From t=0 to t=0.5 sec)	Wind velocity:12m/s $P_{Load} = 5000$ W $P_{Wind} < P_{Load}$ Battery in discharging mode	Wind power is slowly increasing $P_{Battery} = 5368$ W load power is 5000 W (Surplus power 368 W)
Case 2 (From t=1 to t=1.75sec)	Wind velocity:12m/s $P_{Load} = 5000$ W $P_{Wind} > P_{Load}$ Battery in charging mode	Wind power is 5915 W $P_{Battery} = 477$W load power is 5000 W (Surplus power 438 W)
Case 2 (From t=1.75 to t=3.5sec)	Wind velocity:12m/s $P_{Load} = 1500$ W $P_{Wind} > P_{Load}$ Battery in charging mode	Wind power is 5915 W $P_{Battery} = 4041$ W load power is 1500 W (Surplus power 374 W)
Case 2 (From t=3.5 to t=5sec)	Wind velocity:12m/s $P_{Load} = 5000$ W $P_{Wind} > P_{Load}$ Battery in charging mode	Wind power is 5915 W $P_{Battery} = 432$ W load power is 5000 W (Surplus power 483 W)

Figures 18, 19, 20, 21 depict the wind/battery powers, Battery SOC, load power and the DC bus voltage respectively.

Figure 18 depicts the wind power and battery ESS charging/discharging power.

The wind power was precisely tracked based on wind velocity, same as seen in case 1.

The battery offers a reliable energy source to meet the demands of the loads, as seen in Figure 20, a continuous power load (4000 W).

Figure 19 depicts the battery state of charge during charging/discharging mode, the energy storage system is based only on Battery.

Figure 21 depicts the DC-Bus voltage successfully regulated at 350V.

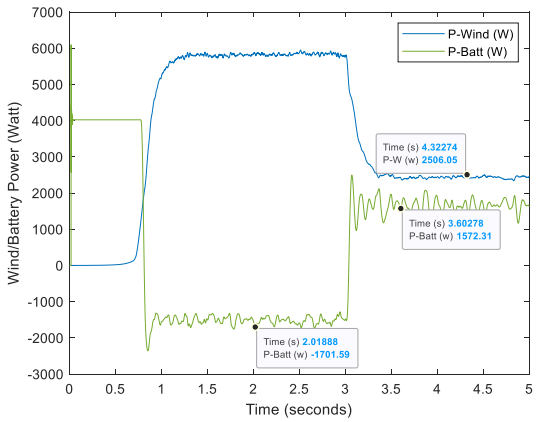

Figure 18. Wind/Battery powers

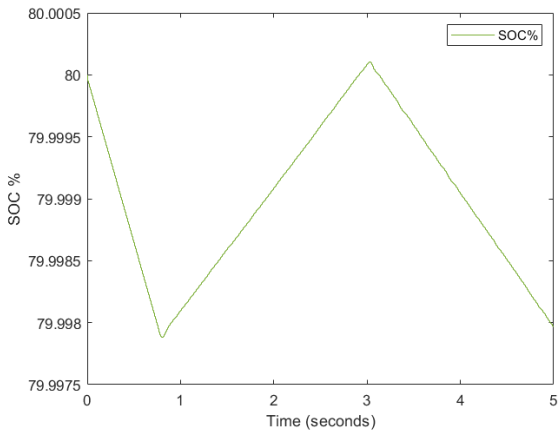

Figure 19. Battery SOC

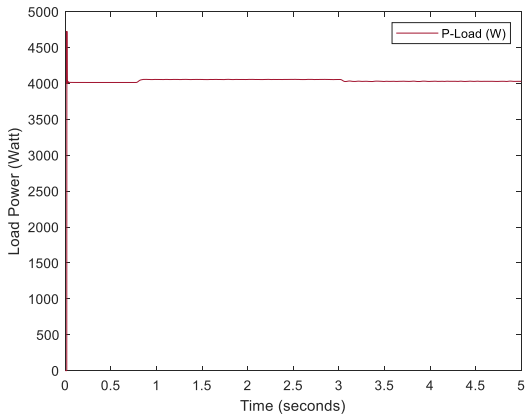

Figure 20. Load power

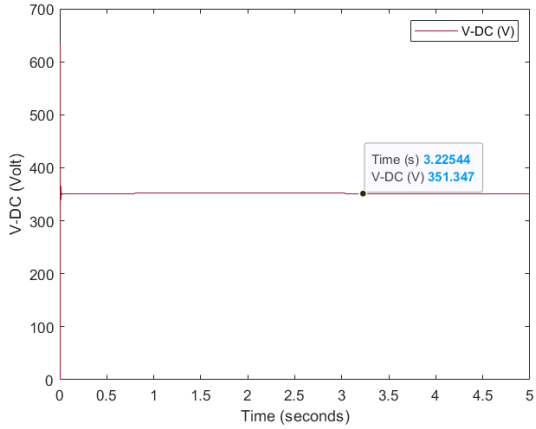

Figure 21. DC-Bus voltage

The analysis of simulation results of wind power generation system and battery (Case 3), are presented in Table 2.

Table 2. The results analysis description (case 3)

Duration	Parameters	Results
Case 3 (From t=0 to t=0.5 sec)	Wind velocity 5m/s $P_{Load} = 4000$ W $P_{Wind} < P_{Load}$ Battery in discharging mode	Wind power is too low $P_{Battery} = 4010$ W Load power is 4000 W (Surplus power 10 W)
Case 3 (From t=1 to t=3sec)	Wind velocity 12m/s $P_{Load} = 4000$ W $P_{Wind} > P_{Load}$ Battery in charging mode	Wind power is 5915 W $P_{Battery} = 1701$ W Load power is 4000 W (Surplus power 214 W)
Case 3 (From t=3.5 to t=5 sec)	Wind velocity 9m/s $P_{Load} = 4000$ W $P_{Wind} < P_{Load}$ Battery in discharging mode	Wind power is 2506 W $P_{Battery} = 1572$W Load power is 4000W (Surplus power 78 W)

In this case, we removed the SCs from the ESS. Batteries have poor charge/discharge rates (low power density), which means that unexpected power fluctuations (the peak transient powers in Figure 18 caused by load power surges or variations in wind speed) interrupt their charge/discharge cycles and eventually shorten their lifetime. In contrast, supercapacitors (SC) have a higher power density, which translates into faster charging/discharging rates and higher efficiency overall.

5. CONCLUSION

An energy management method is presented in this paper for a standalone wind power system generator with hybrid energy storage (HESS) composed of battery and supercapacitor. The latter serves to prevent battery activity in situations having considerable depletion rates. The same DC bus is used to connect both the power sources and the load.

The simulation of the proposed system for various load and wind speed fluctuations indicates that the energy management technique effectively regulates the power flows between the system's components, ensuring power balance at the DC-bus and maintaining voltage stability, all while maximizing wind energy output and preventing battery overcharging.

REFERENCES

[1] Gharibi, M., Askarzadeh, A. (2019). Size optimization of an off-grid hybrid system composed of photovoltaic and diesel generator subject to load variation factor. Journal of Energy Storage, 25: 100814. https://doi.org/10.1016/j.est.2019.100814

[2] IEA, Global Energy. (2019). CO_2 Status Report 2018. International Energy Agency, Paris. https://www.iea.org/reports/global-energy-co2-status-report-2019/renewables.

[3] Gielen, D., Boshell, F., Saygin, D., Bazilian, M.D., Wagner, N., Gorini, R. (2019). The role of renewable energy in the global energy transformation. Energy Strategy Reviews, 23: 38-50. https://doi.org/10.1016/j.esr.2019.01.006

[4] Alshammari, N., Asumadu, J.A. (2020). Optimum unit sizing of hybrid renewable energy system utilizing harmony search, Jaya and particle swarm optimization algorithms. Sustainable Cities and Society, 60: 102255. https://doi.org/10.1016/j.scs.2020.102255

[5] Murphy, C.A., Schleifer, A.H., Eurek, K. (2021). A taxonomy of systems that combine utility-scale renewable energy and energy storage technologies. Renewable & Sustainable Energy Reviews, 139: 110711. https://doi.org/10.1016/j.rser.2021.110711

[6] Rahmanifard, H., Plaksina, T. (2019). Hybrid compressed air energy storage, wind and geothermal energy systems in Alberta: Feasibility simulation and economic assessment. Renewable Energy, 143: 453-470. https://doi.org/10.1016/j.renene.2019.05.001

[7] Notton, G., Mistrushi, D., Mistrushi, D., Stoyanov, L., Berberi, P. (2017). Operation of a photovoltaic-wind plant with a hydro pumping-storage for electricity peak-shaving in an island context. Solar Energy, 157: 20-34. https://doi.org/10.1016/j.solener.2017.08.016

[8] Kadri, A., Marzougui, H., Aouiti, A., Bacha, F. (2020). Energy management and control strategy for a DFIG wind turbine/fuel cell hybrid system with super capacitor storage system. Energy, 192: 116518. https://doi.org/10.1016/j.energy.2019.116518

[9] Hamzaoui, I., Bouchafaa, F., Talha, A. (2016). Advanced control for wind energy conversion systems with flywheel storage dedicated to improving the quality of energy. International Journal of Hydrogen Energy, 41(45): 20832-20846. https://doi.org/10.1016/j.ijhydene.2016.06.249

[10] Firtina-Ertis, I., Acar, C., Erturk, E. (2020). Optimal sizing design of an isolated stand-alone hybrid wind-hydrogen system for a zero-energy house. Applied Energy, 274: 115244. https://doi.org/10.1016/j.apenergy.2020.115244

[11] Ghaffarzadeh, H., Mehrizi A. (2020). Review of control techniques for wind energy systems. Energies, 13(24): 6666. https://doi.org/10.3390/en13246666

[12] Elyaalaoui, K., Ouassaid, M., Cherkaoui, M. (2018). Primary frequency control using hierarchal fuzzy logic for a wind farm based on SCIG connected to electrical network. Sustainable Energy, Grids and Networks, 16: 188-195. https://doi.org/10.1016/j.segan.2018.07.008

[13] Arani, A.A., Karami, H., Gharehpetian, G.B., Hejazi, M.A. (2017). Review of flywheel energy storage systems structures and applications in power systems and microgrids. Renewable & Sustainable Energy Reviews, 69: 9-18. https://doi.org/10.1016/j.rser.2016.11.166

[14] Oh, E., Son, S. (2020). Theoretical energy storage system sizing method and performance analysis for wind power forecast uncertainty management. Renewable Energy, 155: 1060-1069. https://doi.org/10.1016/j.renene.2020.03.170

[15] Errouissi, R., Al-Durra, A., Debouza, M. (2018). A novel design of PI current controller for PMSG-based wind turbine considering transient performance specifications and control saturation. IEEE Transactions on Industrial Electronics, 65: 8624-8634. https://doi.org/10.1109/TIE.2018.2814007

[16] Mendis, N., Muttaqi, K.M., Perera, S. (2014). Management of battery-supercapacitor hybrid energy storage and synchronous condenser for isolated operation of PMSG based variable-speed wind turbine generating systems. IEEE Transactions on Smart Grid, 5(2): 944-953. https://doi.org/10.1109/TSG.2013.2287874

[17] Pan, T.L., Wan, H.S., Ji, Z.C. (2014). Stand-alone wind power system with battery/supercapacitor hybrid energy storage. International Journal of Sustainable Engineering, 7(2): 103-110. https://doi.org/10.1080/19397038.2013.779327

[18] Fahmi, M.I., Rajkumar, R.K., Arelhi, R., Isa, D. (2015). Study on the effect of supercapacitors in solar PV system for rural application in Malaysia. 2015 50th International Universities Power Engineering Conference (UPEC), pp. 1-5. https://doi.org/10.1109/UPEC.2015.7339921

[19] Zakzouk, N.E., Lotfi, R.A. (2020). Power flow control of a hybridbattery/supercapacitor Standalone PV System under Irradiance and Load Variations. 10th International Conference on Power and Energy Systems (ICPES), pp. 469-474.

[20] Mansour, M., Mansouri, M.N., Bendoukha, S., Mimouni, M.F. (2020). A grid-connected variable-speed wind generator driving a fuzzy-controlled PMSG and associated to a flywheel energy storage system. Electric Power Systems Research, 180: 106137. https://doi.org/10.1016/j.epsr.2019.106137

[21] Trejos-Grisales, L.A., Guarnizo–Lemus, C., Serna, S. (2014). Overall Description of Wind Power. Ingeniería y Ciencia, 10(19): 99-126. https://doi.org/10.17230/ingciencia.10.19.5

[22] Hind, E., NoureddineELmouhi, Essadki, A., Chakib, R. (2022). Comparative study of power smoothing techniques produced by a wind energy conversion system. International Journal of Electrical and Computer Engineering Systems, 13(1): 77-86. https://doi.org/10.32985/ijeces.13.1.8

[23] Pan, L., Shao, C. (2020). Wind energy conversion systems analysis of PMSG on offshore wind turbine using improved SMC and Extended State Observer. Renewable Energy, 161: 149-161. https://doi.org/10.1016/j.renene.2020.06.057

[24] Thapa, K.B., Jayasawal, K. (2020). pitch control scheme for rapid active power control of a PMSG-Based wind power plant. IEEE Transactions on Industry Applications, 56(6): 6756-6766. https://doi.org/10.1109/TIA.2020.3015169
[25] Amirante, R., Cassone, E., Distaso, E., Tamburrano, P. (2017). Overview on recent developments in energy storage: Mechanical, electrochemical and hydrogen technologies. Energy Conversion and Management, 132: 372-387. https://doi.org/10.1016/j.enconman.2016.11.046
[26] Babazadeh, H., Gao, W., Lin, J., Cheng, L. (2012). Sizing of battery and supercapacitor in a hybrid energy storage system for wind turbines. PES T&D 2012, 1-7. https://doi.org/10.1109/TDC.2012.6281704
[27] Jayalakshmi, N.S., Nempu, P.B. (2021). Performance enhancement of a hybrid AC-DC microgrid operating with alternative energy sources using supercapacitor. International Journal of Electrical and Computer Engineering Systems, 12(2): 67-76. https://doi.org/10.32985/ijeces.12.2.1
[28] Thakur, A., Saini, M. (2015). A new control scheme for battery-supercapacitor hybrid energy storage system for standalone photovoltaic application. International Journal of Engineering, Management & Sciences, 2(5): 25-32.

NOMENCLATURE

W_r	The turbine angular speed
ρ	The air density
β	The pitch angle
λ	The tip speed ratio
R_s	The resistance of the stator winding
C_p	The power coefficient
V_{sd},V_{sq}	The stator voltages
i_d , i_q	Direct and quadrature current comps.
L_{sd}, L_{sq}	d-q axis Inductances
λ_m	The core magnetic flux
T_e	The PMSG electrical torque
V_{DC}	DC link voltage
$P_{Bat/SC}$	Battery/SCs power
P_W	The wind power
P_L	The load power